Conceptual Data Sampling For Breast Cancer Histology Image Classification

Eman Rezk[a], Zainab Awan[a], Fahad Islam[a], Ali Jaoua[a,1], Somaya Al Maadeed[a],

Nan Zhang[b], Gautam Das[c], Nasir Rajpoot[d]

[a] Department of Computer Science and Engineering, Qatar University, Qatar

[b] Department of Computer Science, George Washington University, USA

[c] Department of Computer Science and Engineering, University of Texas at Arlington, USA

[d] Department of Computer Science, University of Warwick, UK

[1] Corresponding author email address: jaoua@qu.edu.qa

Abstract

Data analytics have become increasingly complicated as the amount of data has increased. One technique that is used to enable data analytics in large datasets is data sampling, in which a portion of the data is selected to preserve the data characteristics for use in data analytics. In this paper, we introduce a novel data sampling technique that is rooted in formal concept analysis theory. This technique is used to create samples reliant on the data distribution across a set of binary patterns. The proposed sampling technique is applied in classifying the regions of breast cancer histology images as malignant or benign. The performance of our method is compared to other classical sampling methods. The results indicate that our method is efficient and generates an illustrative sample of small size. It is also competing with other sampling methods in terms of sample size and sample quality represented in classification accuracy and F1 measure.

Keywords: Data sampling; Formal concept analysis; Image segmentation; Breast cancer classification; histopathology.

1. Introduction

Breast cancer is one of the most common cancers in women in the world, and it represents 25% of the overall cancers. Statistics indicate that every 60 seconds, somewhere in the world, someone dies from breast cancer. With this rate, it is expected that 13 million breast cancer deaths will occur in the world in the coming 25 years. Breast cancer can be treated if it is diagnosed in its early stages [1]. The breast cancer histology images are processed through certain image filters to produce a set of features describing each pixel. This process generates a massive amount of data that needs to be analyzed in order to classify the pixels as malignant or benign. It is here that the importance of sampling arises to take a discriminative set of the data to be used in the classification process.

The objective of any data sampling technique is to extract a portion of the data that preserves data behavior while reducing sampling cost and error [2]. In this paper, a new data sampling method is proposed and employed in classifying breast cancer images. This method is rooted in formal concept analysis (FCA) theory, which is a mathematical framework used for conceptual data analysis, in which data are represented as a binary relation that links tuples and features [3]. This binary relation is transformed into a set of binary patterns, which is then used to select a sample from the data while preserving patterns proportions across the data.

The novelty of the sampling method is due to several factors: 1) it considers all data features while generating patterns, unlike other existing sampling methods that consider only one feature; 2) it considers data distribution among different patterns to generate proportional samples that represent the real distribution of data; 3) it does not require any prior knowledge about the data.

The proposed method is validated and evaluated against two of the most widely used sampling algorithms: simple random sampling and stratified sampling. All sampling methods are validated using a machine-learning case study of breast cancer image classification. The samples are fed into different algorithms which build several classifiers to detect whether the pixels are malignant or benign, and evaluated using classification accuracy and F1 measure.

The paper is organized as follows; section 2 introduces some background information. Section 3 explains the methodology including image processing, sampling and learning steps. In section 4, the data set, experimental setup, and experimental results are discussed. Finally, we conclude our work.

2. Background

In this section, the backgrounds of the topics examined in the subsequent sections are described in detail.

2.1 Formal Concept Analysis

FCA is a mathematical framework built on lattice theory that provides data analysis and knowledge discovery [3]. It works by analyzing the binary relations between tuples and features [4]. FCA is a beneficial data analysis technique that has been widely applied in different fields such as feature reduction [5], image mining [6], and decision-making [7].

In FCA, the main entity is a binary relation that is called a formal context, which is defined as follows: A formal context (FC) is a triplet k = <O,A,I>, where O and A represent objects and attributes respectively. The binary relation defined between O and A is noted as I and the term I(o, a) means the value of object o in attribute a [8], [9], [10].

Table 1 provides an example of a formal context with O = {Lion, Finch, Eagle, Hare, Ostrich}, A = {Preying, Flying, Bird, Mammal} and I (Finch, Bird) = 1.

Table 1. Example of a formal context

	Preying	Flying	Bird	Mammal
Lion	1	0	0	1

Finch	0	1	1	0
Eagle	1	1	1	0
Hare	0	0	0	1
Ostrich	0	0	1	0

2.2 Sampling Methods

One way to overcome the data size problem is data sampling, which is the process of drawing a sample from a population that helps in making inferences. The process of drawing a sample is shown in Fig. 1. The accuracy of the analytics performed using only samples of the data is extensively based on the quality of the selected samples. Therefore, the sampling design plays a crucial role in both the sampling process and the inference process. As the sampling design provides the method used to collect the sample, it should be accurate, efficient, and feasible [11]. In this paper, we use simple random sampling and stratified sampling for their simplicity and efficiency.

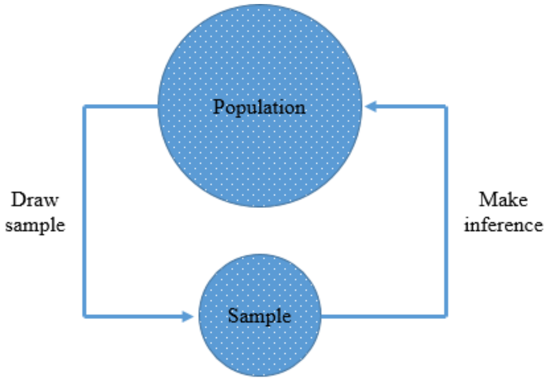

Fig. 1. Data sampling process

2.2.1 Simple Random Sampling (SRS)

All elements in the population have equal probability of being selected for the sample. SRS is easy to implement and it can be used to estimate the population total and mean. The mean is unbiased and sample variance can be estimated using a single sample. However, it is not efficient enough [12], [13].

2.2.2 Stratified Sampling

In stratified sampling, the population is divided into non-overlapping groups based on certain known criteria such as age, gender, or country. This set of groups is called strata, and each subgroup is called a stratum. A sample is drawn randomly from each stratum [14]. The process of stratified sampling is shown in Fig. 2.

Stratified sampling helps in understanding the problem domain and in producing representative samples that enhance sample estimates and reduce sampling error. Moreover, it enables the analysis of each subgroup by providing separate estimates. Stratified sampling is more efficient than SRS particularly when the points of each stratum are homogenous and the points between strata are heterogeneous [14], [15].

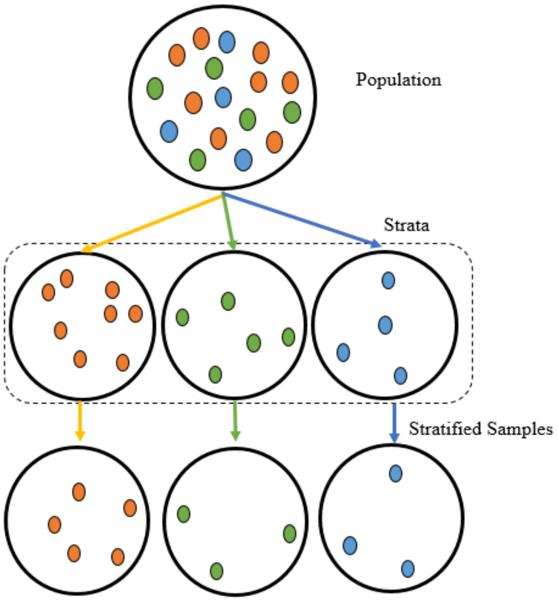

Fig. 2. Stratified sampling

2.3 Image Segmentation

Image segmentation is the process of partitioning an image into a set of pixels based on color, intensity, and texture [16]. Image segmentation plays a crucial role in cancer detection and severity evaluation, Fig. 3 shows an example of a breast cancer image that is segmented to identify the tumor regions. It helps in restricting the analysis process to areas containing tumor cells only and avoids any confusion with other regions. Image segmentation is definitely a challenging problem due to the enormous amount of inconsistencies in the images. Image inconsistency may arise from the differences in images collection such as noise, cut consistency, dye concentration, and slide scanners [17].

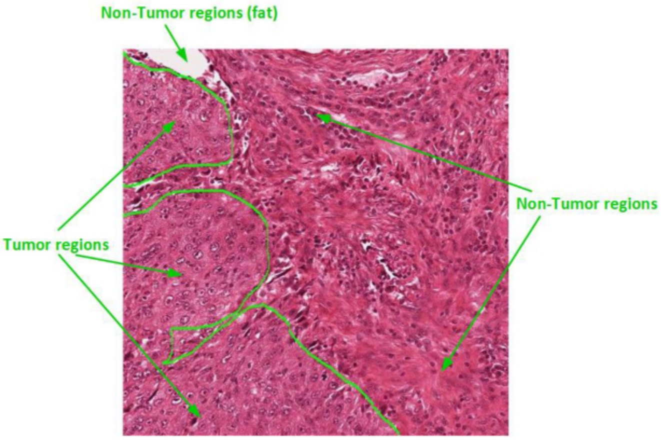

Fig. 3. Breast cancer image segmentation [16]

Numerous methods are developed to segment the images. In [16], breast cancer images segmentation is represented as a machine learning problem that is solved using supervised and unsupervised learning methods. Gurcan et al. in [18] target segmenting the hematoxylin and eosin (H&E) stained images to classify a pediatric nervous system cancer. They integrated the top hat and thresholding algorithms to segment the cell nuclei. Cosatto et al. provide a high accuracy classifier for breast cancer nuclear segmentation and grading [19]. Yang et al. segment the blood cancer histopathology specimens by constructing a concave vertex graph. This graph is based on employing a contouring model to define the concave boundary points and inner edges [20]. For breast cancer images of tissue microarrays, Qi et al. succeeded in accurately segmenting overlapped cells. Their model started by finding the object centers, then clustering, and finally contouring the cells [21].

In [22], the authors work on breast and cervix image segmentation. The watershed algorithm is used to extract nuclei, while the oversegmentation problem is tackled using a novel marker extraction schema. Ali and Madabhushi [23] investigate the limitations of the classical active contouring algorithm to segment the highly overlapped objects of breast and prostate tissues. Their proposed technique is able to generate better boundary separations and handle object occlusion. In [24], a framework for classifying breast cancer image pixels as tumor or stromal regions is proposed. The image is split into four regions: tumor, Hypocellular stroma, Hypercellular stroma, and fat that is removed during the preprocessing step. The texture features of the hypo and hyper stroma are extracted using different orientations of a Gabor filter.

The emergence of deep learning helped the improvement of image segmentation and analysis. Sirinukunwattana et al. [25] propose an integrated framework for nuclei detection and classification that is based on deep learning techniques. A convolutional neural network is mainly employed for both detection and classification. In [26], the authors employ a convolutional neural network to solve the problem of classifying unbalanced data of breast cancer images. The proposed framework segments the images, and then recognizes the non-mitotic parts of the image that are later under sampled, while oversampling the mitotic parts to achieve the balance between the classes.

3. Methodology

The work proposed is mainly divided into three main parts; the image processing, the sampling, and the learning. In image processing, the image quality is improved and features are extracted as indicated in section 3.1. The sampling is the main contribution of this paper that is explained in detail in section 3.2. The learning process aims to build several classifiers using different classification algorithms that are trained from the samples. The learning process is explained in detail in section 3.3.

In Fig. 4, image (A) shows the original breast cancer image, while image (B) is the predicted one resulting after the learning process; the white regions represent the tumors and the black regions are the normal cells.

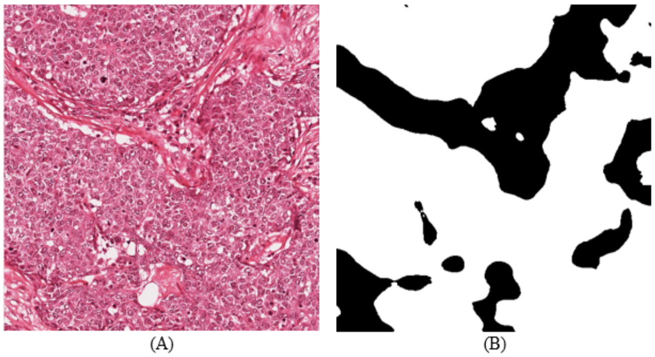

Fig. 4. Example of the original breast cancer image (A) and the predicted one (B)

3.1 Image Processing

In image processing, the image quality is improved through: 1) stain normalization, 2) conversion to gray scale, and 3) noise removal.

Stain normalization targets the color consistency, so it corrects the color inconsistency of breast cancer images resulting from light, scanner type, and stain variations from one laboratory to another. Fig. 5 shows the effect of stain normalization on breast cancer images, figures A and B are the images before stain normalization, while figures C and D are after stain normalization. A plethora of stain normalization algorithms are available. In [27–29] the histogram specification technique is used because it discriminates between the tumor and the non-tumor parts clearly.

The stained images are converted to grey scale using MATLAB[2]. Then, the noise in the images is removed by smoothing the image brightness using a smoothing Gaussian filter that fits the image distribution, Fig. 6 illustrates a source colored breast cancer image (A) and a preprocessed image after stain normalization, grey scale conversion, and noise removal (B).

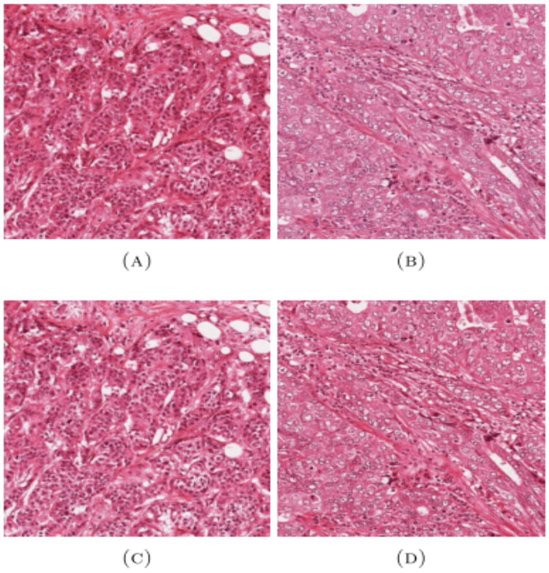

Fig. 5. Illustration of stain normalization on breast cancer images [16]

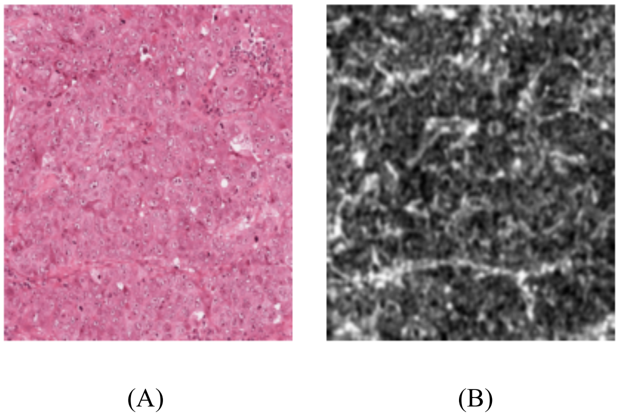

[2] http://www.mathworks.com/help/images/ref/rgb2lab.html

Fig. 6. The difference between the source and preprocessed image [16]

After preprocessing images, a feature extraction step is performed. Features represent the characteristics of the images. In this work only the textural features are extracted to minimize color and intensity dependencies. Textural features depend on the structure and the pattern of the tumor regions and hence, they are dominant in determining the tumor and non-tumor regions of an image.

Several techniques can be used to extract textural features such as Maximum Response 8 (MR8) filter bank [30], Root Filter Set (RFS) bank [31], and Haralick filter [32]. In this work, we focus on the MR8Fast filter that is derived from the MR8 filter bank. It extracts 8 responses only, so each image has 8 features.

3.2 The Proportional Sampling

The proposed pattern-based proportional sampling method (PPS) is centered on the representation of conceptual data. First, the input dataset is transformed into a binary relation called a formal context. This relation is mapped into binary patterns and then, a proportion of each pattern is calculated and converted back to the original data. Fig. 7 shows the steps in the method, which are explained in detail in the following sections.

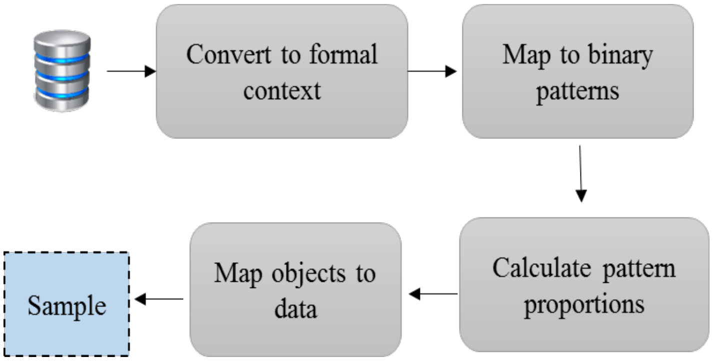

Fig. 7. Proposed sampling method

A. Convert Data to Formal Context

Data are converted to the formal context by performing pairwise comparisons between data tuples as in [33]. Fig. 8 shows the example of a database instance (DBI) that is transformed into a formal context. Tuples T_1 and T_2 are compared for attributes A, B, C, and D. This comparison is translated into a new object in the FC with the same attributes containing “0” if the values are not equal and “1” otherwise. Tuple T_1(A) is not equal to T_2(A); hence, (T_1,T_2) (A) in the FC is “0”. However, T_1(B) = T_2(B), so (T_1,T_2) (B) in the FC is “1”.

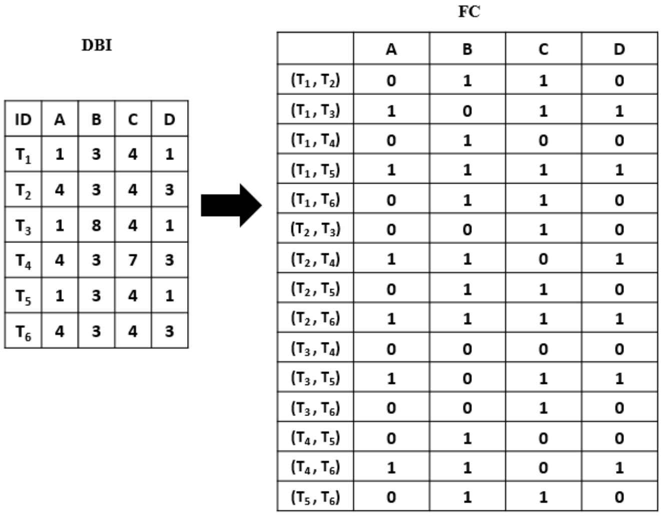

DBI

ID	A	B	C	D
T_1	1	3	4	1
T_2	4	3	4	3
T_3	1	8	4	1
T_4	4	3	7	3
T_5	1	3	4	1
T_6	4	3	4	3

FC

	A	B	C	D
(T_1, T_2)	0	1	1	0
(T_1, T_3)	1	0	1	1
(T_1, T_4)	0	1	0	0
(T_1, T_5)	1	1	1	1
(T_1, T_6)	0	1	1	0
(T_2, T_3)	0	0	1	0
(T_2, T_4)	1	1	0	1
(T_2, T_5)	0	1	1	0
(T_2, T_6)	1	1	1	1
(T_3, T_4)	0	0	0	0
(T_3, T_5)	1	0	1	1
(T_3, T_6)	0	0	1	0
(T_4, T_5)	0	1	0	0
(T_4, T_6)	1	1	0	1
(T_5, T_6)	0	1	1	0

Fig. 8. Converting database instance into a formal context

One drawback of this transformation method is the exact matching between numbers, which allows for information loss. To overcome this problem, a similarity measure is introduced to perform the pairwise comparison process as discussed in [33]. It is calculated as follows:

$$Similarity = \left[1 - \frac{|n1 - n2|}{\max(n1, n2)}\right] \qquad (1)$$

where n_1, n_2 are the two numbers.

In this step, the percentage of similarity is calculated during the pairwise comparison. If the similarity between the data values is greater than a certain threshold, then the FC object value is “1”; otherwise the value of the FC object is “0”.

B. Map to Binary Patterns

A set of binary patterns is generated based on the number of features in the FC which is the same as the number of features of the dataset. A formal context with *M* features has a binary pattern table of size 2^M patterns. Each FC object is mapped to one of these patterns and a counter attached to each pattern is incremented. Only a fixed number of FC objects is stored for each pattern to minimize memory usage. Examples of a binary pattern table (PT) and the counter table (CT) generated for a FC with four attributes are illustrated in Fig. 9. For example, since objects (T_2, T_3) and (T_3, T_6) are mapped to pattern “0010”, its corresponding counter value in the CT is 2.

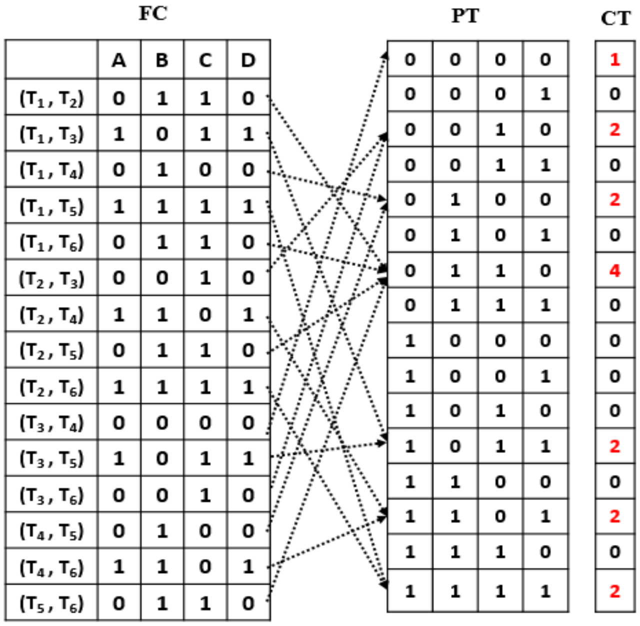

FC

	A	B	C	D
(T_1, T_2)	0	1	1	0
(T_1, T_3)	1	0	1	1
(T_1, T_4)	0	1	0	0
(T_1, T_5)	1	1	1	1
(T_1, T_6)	0	1	1	0
(T_2, T_3)	0	0	1	0
(T_2, T_4)	1	1	0	1
(T_2, T_5)	0	1	1	0
(T_2, T_6)	1	1	1	1
(T_3, T_4)	0	0	0	0
(T_3, T_5)	1	0	1	1
(T_3, T_6)	0	0	1	0
(T_4, T_5)	0	1	0	0
(T_4, T_6)	1	1	0	1
(T_5, T_6)	0	1	1	0

PT				CT
0	0	0	0	1
0	0	0	1	0
0	0	1	0	2
0	0	1	1	0
0	1	0	0	2
0	1	0	1	0
0	1	1	0	4
0	1	1	1	0
1	0	0	0	0
1	0	0	1	0
1	0	1	0	0
1	0	1	1	2
1	1	0	0	0
1	1	0	1	2
1	1	1	0	0
1	1	1	1	2

Fig. 9. Mapping FC objects to patterns

C. Calculate Pattern Proportions

After mapping all FC objects to their corresponding patterns, the CT indicates the frequencies of each pattern across all the data. Each value in the CT is divided by the total number of objects in the formal context to obtain the proportion of each pattern. This proportion is multiplied by a multiplier *K* where *K* > 0. It controls the number of objects to be sampled from each pattern. The higher the multiplier value, the bigger the sample size. It is calculated as follows:

$$Pattern\ Proportion = \frac{CT\ (pattern)}{Number\ of\ FC\ objects} \qquad (2)$$

$$Pattern\ Sample\ Count = \ Pattern\ proportion \times K \qquad (3)$$

A number of objects is selected from each pattern based on its calculated sample size. For example, a pattern sample count of 10 means that the first 10 objects belonging to this pattern are selected as the sample.

D. Map Objects to Original Data

The pattern sample size provides statistical information about the tuples in the original database. Patterns with higher proportions have higher numbers of FC objects and thus, more objects are sampled from them while patterns with low proportions and zero sample size are not included in the sample. This mapping process significantly empowers our sampling method because it recognizes the outliers and data distribution in different patterns without prior knowledge about the data.

The sampled FC objects are mapped to the tuples in the original database to generate the sample. For example, in Fig. 10, the pattern {0110} has four objects {(T_1, T_2), (T_1, T_6), (T_2, T_5) and (T_5, T_6)}. In this example, the multiplier is 7 to get a very small sample because the dataset is already fairly small. The pattern sample size for {0110} is 1.87, which can be rounded to 2 for the sample count, so two FC objects are randomly selected from this pattern. Assume that FC objects {(T_1, T_2) and (T_1, T_6)} are sampled from the FC. Therefore, the tuples T_1, $T_{2,}$ and T_6 are selected from the original dataset in the sample. This process is repeated for all patterns that have sample counts greater than zero.

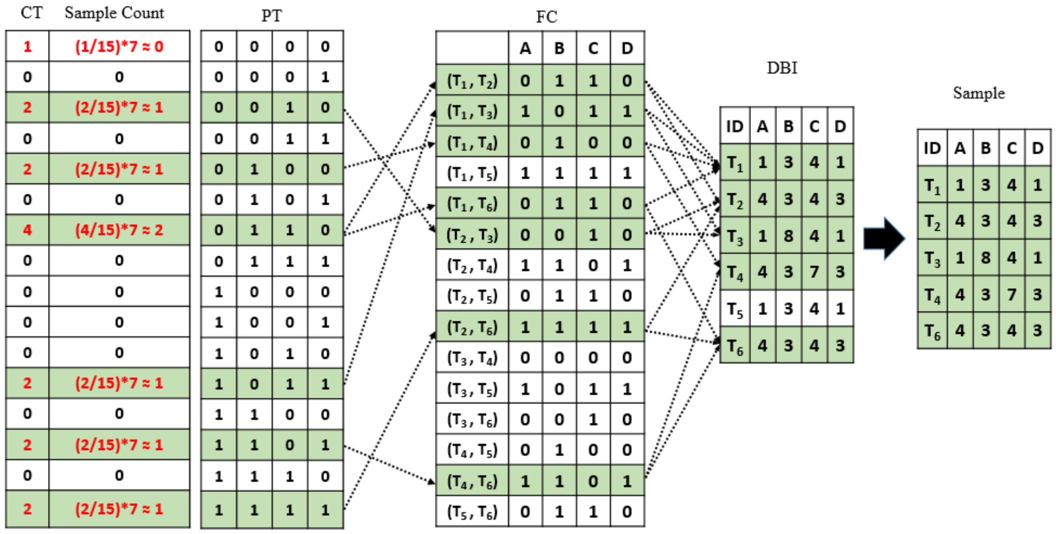

CT	Sample Count
1	(1/15)*7 ≈ 0
0	0
2	(2/15)*7 ≈ 1
0	0
2	(2/15)*7 ≈ 1
0	0
4	(4/15)*7 ≈ 2
0	0
0	0
0	0
0	0
2	(2/15)*7 ≈ 1
0	0
2	(2/15)*7 ≈ 1
0	0
2	(2/15)*7 ≈ 1

PT

0	0	0	0
0	0	0	1
0	0	1	0
0	0	1	1
0	1	0	0
0	1	0	1
0	1	1	0
0	1	1	1
1	0	0	0
1	0	0	1
1	0	1	0
1	0	1	1
1	1	0	0
1	1	0	1
1	1	1	0
1	1	1	1

FC

	A	B	C	D
(T_1, T_2)	0	1	1	0
(T_1, T_3)	1	0	1	1
(T_1, T_4)	0	1	0	0
(T_1, T_5)	1	1	1	1
(T_1, T_6)	0	1	1	0
(T_2, T_3)	0	0	1	0
(T_2, T_4)	1	1	0	1
(T_2, T_5)	0	1	1	0
(T_2, T_6)	1	1	1	1
(T_3, T_4)	0	0	0	0
(T_3, T_5)	1	0	1	1
(T_3, T_6)	0	0	1	0
(T_4, T_5)	0	1	0	0
(T_4, T_6)	1	1	0	1
(T_5, T_6)	0	1	1	0

DBI

ID	A	B	C	D
T_1	1	3	4	1
T_2	4	3	4	3
T_3	1	8	4	1
T_4	4	3	7	3
T_5	1	3	4	1
T_6	4	3	4	3

Sample

ID	A	B	C	D
T_1	1	3	4	1
T_2	4	3	4	3
T_3	1	8	4	1
T_4	4	3	7	3
T_6	4	3	4	3

Fig. 10. Sampling from DBI based on pattern proportion

3.3 The Learning Process

The generated samples are used to classify the image pixels as malignant or benign. This is achieved by a machine learning process based on 5 classification algorithms: naïve Bayes (NB), support vector machine (SVM), pattern net (PN), cascade forward net (CFN), and feed forward net (FFN) using the statistics and machine learning toolbox of MATLAB[3].

[3] https://www.mathworks.com/products/statistics.html

The training set is the sample and the test set is not previously known to the classifier. The classification accuracy and F1 measure [34] are reported to evaluate the samples and the learning process. In addition, our sampling method is compared to the classical sampling methods; simple random sampling (SRS) and stratified sampling (SS). All the generated samples are used through the learning process for validation and evaluation.

4. Results and Discussion

In this section, we discuss the experiments performed on the breast cancer images of the MITOS 2012 dataset[4]. It contains 50 images from 5 patients and each image has 512 × 512 pixels and 8 features that are labelled (malignant or benign) manually by domain experts. The experimental setup section explains the configurations of each group of experiments; the data split and cross validation results sections show the results achieved using the clarified configurations.

4.1 Experimental Setup

Two main groups of experiments are performed, the data split group and the cross-validation group. In the data split experiments, the 50 images are divided into 2 equal sized partitions. A random sample of size 10,000 pixels is selected from the first partition that includes 25 images (400 pixels from each image) and given as input for all sampling methods. The second partition with the other 25 images is used for testing with a total size of 6,553,600 (512 x 512 x 25) pixels. The proposed sampling method, PPS is configured with 70%, 80%, and 90% similarity thresholds to study their effects on the sample quality. Also the multiplier is tuned to 100 and 1000 to produce different sample sizes. On the other

[4] http://ipal.cnrs.fr/ICPR2012

hand, SRS and SS methods are tested for sample sizes of 200 and 1500. The results of the data split experiments are discussed in section 4.2.

In the cross-validation group, the images are subdivided into 10 sets of 5 images. From each image, a smaller sample of 750 rows is randomly selected, thus, each subset has a total sample size of 3750(750*5) rows. Since we are doing 10-fold cross-validation, 9 subsets are used for training while one is used for testing and the input to PPS is the 9 subsets combined into a single dataset totaling 33,750 rows. The PPS similarity threshold is tuned to 70%, 80%, and 90% just like in the previous experiment while the multiplier is set to 1000 to have sufficient sample size. On the other hand, SRS and SS are configured with a sample size of 1200 rows. The results of the cross-validation experiments are discussed in section 4.3.

4.2 Data Split Results

In PPS, the similarity threshold affects the sample size. Fig. 11 shows that the sample size increases with the increase in similarity threshold for both the 100 and 1000 multipliers. This is because the higher the similarity threshold, the lower the number of ones in the FC and hence more tuples are needed to preserve data characteristics.

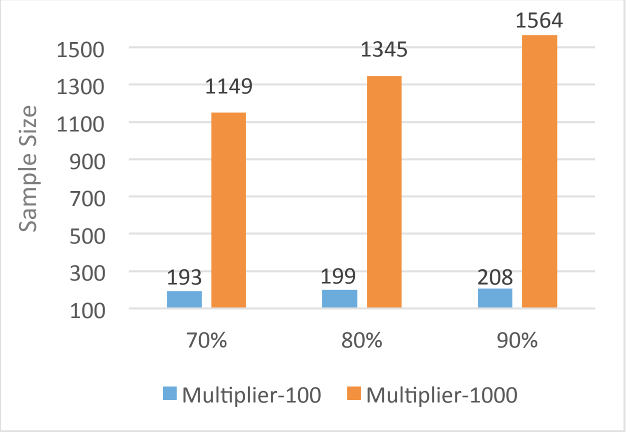

Fig. 11. Sample size with all similarity thresholds and multipliers

The comparison of the algorithms using different similarity thresholds and multiplier-100 are shown in Fig. 12 and Fig. 13. SVM outperforms other algorithms especially for the 70% similarity threshold sample that leads in terms of accuracy and F1 measure.

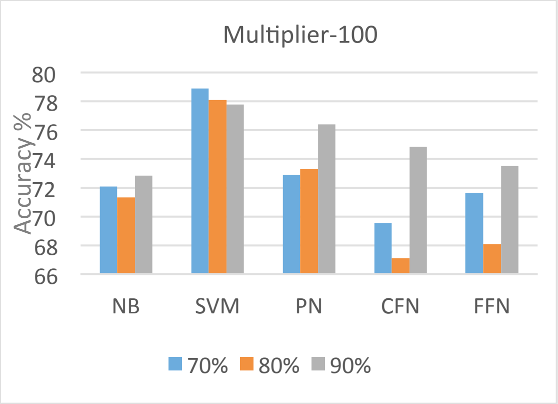

Fig. 12. Accuracy of all algorithms and similarity thresholds

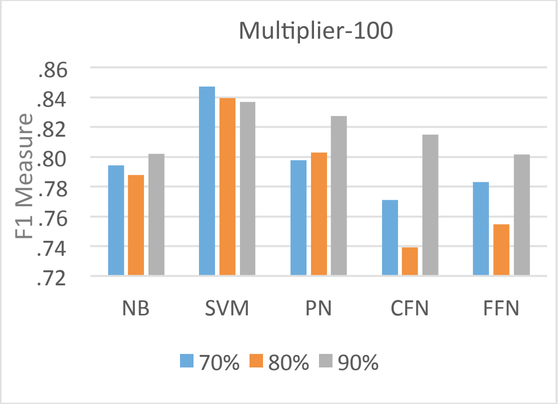

Fig. 13. F1 of all algorithms and similarity thresholds

In addition, we also compared the accuracy and F1 measure using multiplier-1000 that are represented in Fig. 14 and Fig. 15. Here also, SVM outperforms all other algorithms but the differences in accuracy and F1 measure are not significant across the three similarity thresholds.

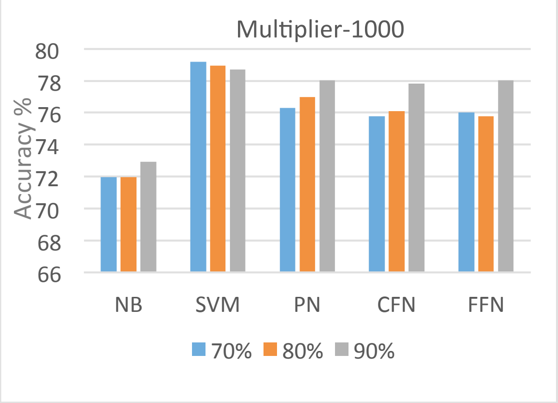

Fig. 14. Accuracy of different algorithms and similarity thresholds

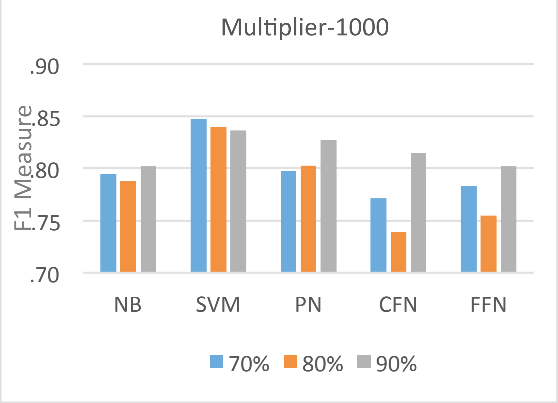

Fig. 15. F1 Measure of different algorithms and similarity thresholds

Fig. 16 and Fig. 17 compare PPS with other sampling methods in terms of classification accuracy using the smaller and bigger sample sizes respectively. Fig. 18 and Fig. 19 represent the F1 measure using the smaller and bigger sample sizes. It is clear that PPS-100 is outperforming SRS-200 and SS-200. Also, the accuracy of PPS-1000 is better than SRS-1500 and SS-1500. In addition, we also noticed the trend that the accuracy of all sampling methods improves with the increase in sample size. PPS-1000 gives the best accuracy and F1 measure when compared to SRS and SS using samples of size 200 and 1500. For example, PPS-100 using SVM achieved 78.9% accuracy with sample size 193 compared to 77% for SRS-1500 and 77.1% for SS-1500. Moreover, the F1 measure graph also shows that PPS is better than other methods. For example, using SVM, PPS-100 achieves 0.85 F1 measure with 193 sample size, while SRS-1500 and SS-1500 have an F1 measure of 0.83.

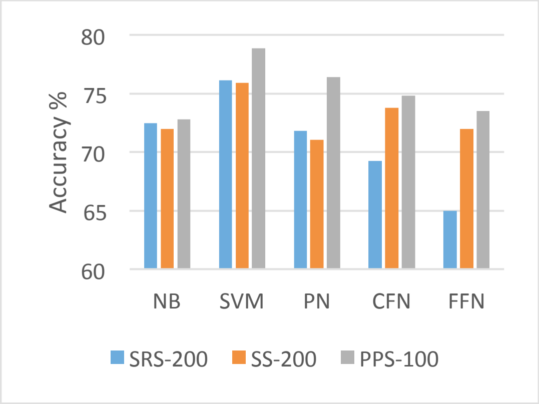

Fig. 16. Accuracy of all sampling methods using the smaller sample size

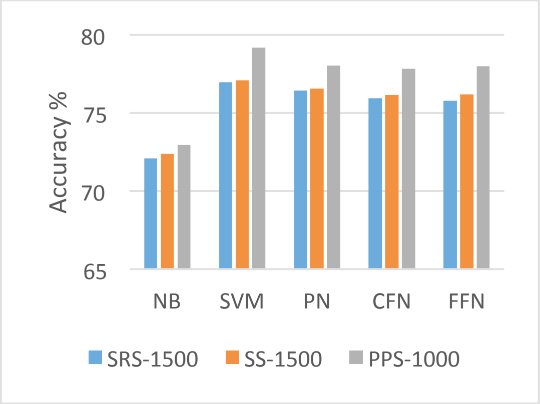

Fig. 17. Accuracy of all sampling methods using the bigger sample size

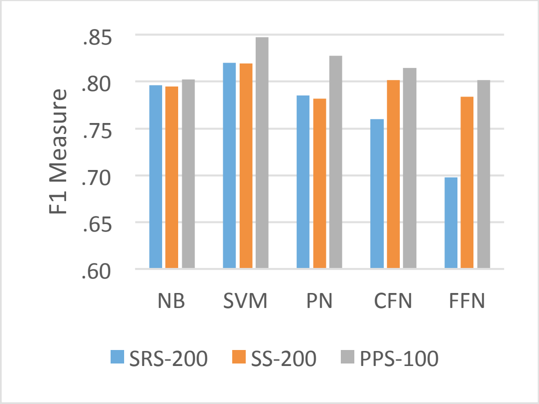

Fig. 18. F1 measure of all sampling methods using the smaller sample size

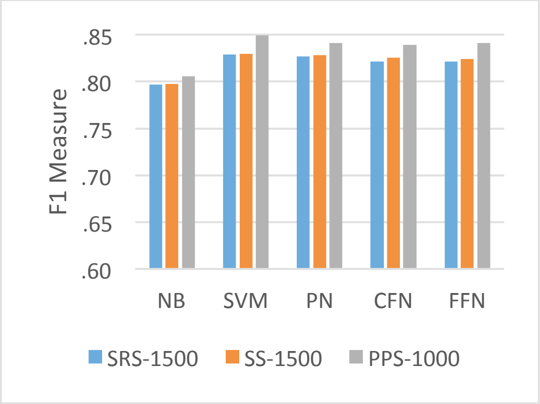

Fig. 19. F1 measure of all sampling methods using the bigger sample size

4.3 Cross Validation Results

The comparison of the classification accuracy using different similarities and algorithms are shown in Fig. 20. The 90% similarity threshold results in the best classification accuracy for all algorithms while SVM outperforms all other algorithms with 78% accuracy. The F1 measure graph is shown in Fig. 21. It also confirms that the 90% similarity threshold is the best for this set of experiments. Also, SVM is achieving the best F1 measure with 0.84.

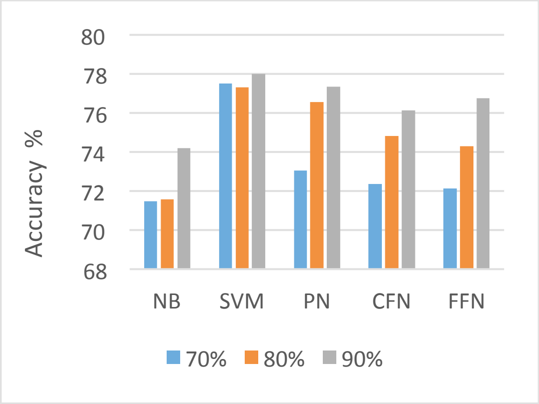

Fig. 20. Accuracy of the cross validation process

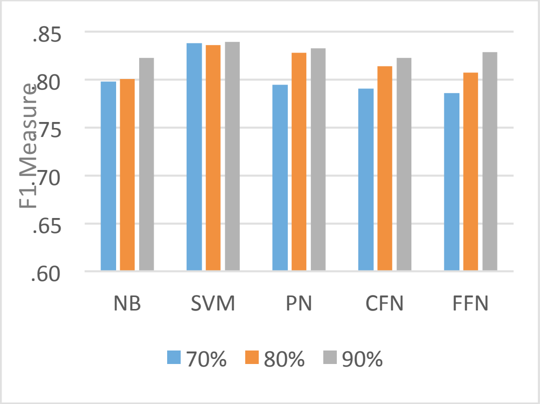

Fig. 21. F1 measure of the cross validation process

In Fig. 22, we compare PPS with SRS and SS. We see that our proposed method is competing with the other sampling methods. SVM results in the highest accuracy compared to other classification algorithms with a value of 78%. In the F1 measure graph shown in Fig. 23, using NB algorithm, the PPS method is outperforming other methods. While using SVM, there is a slight difference in F1 measure between all the methods; SRS has value of 0.845, SS has 0.843, and PPS has 0.839.

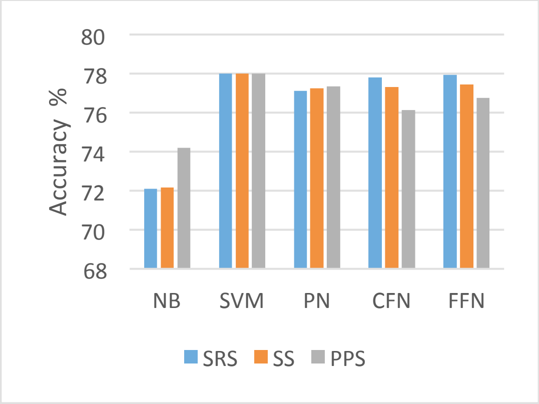

Fig. 22. Accuracy of PPS against SRS and SS with the cross validation process

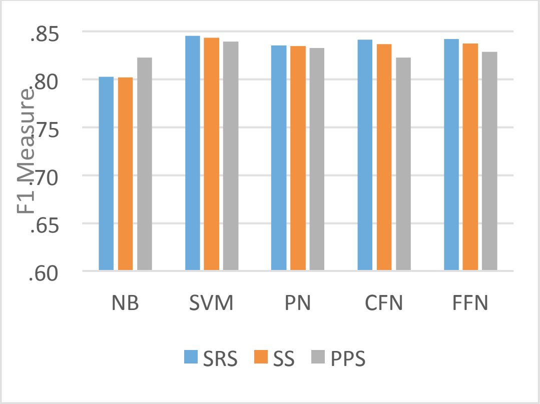

Fig. 23. F1 measure of PPS against SRS and SS with the cross validation process

4.4 Comparison with Other Methods

The proposed sampling method is compared to the SRS and SS. The results show that the PPS method is competing with the other techniques using different machine learning algorithms. In some cases, PPS is not outperforming SRS or SS especially when using CFN and FFN. For example, in Fig. 23 the F1 measure for PPS using FFN is 0.83 while SRS and SS have F1 measure of 0.84. This situation happens because of the lack of randomization when selecting the samples from the patterns. On the other hand, both SRS and SS employ randomization that can significantly improve the accuracy of methods that suffer from local minima and poor generalization, such as neural networks [35]. Moreover, SS can only be applied after analyzing the whole dataset and deciding the stratification parameters and stratum sizes whereas, both PPS and SRS don't need any prior knowledge about the dataset.

In terms of complexity, considering an input dataset of N tuples and M features, the space complexity of our PPS method is $Min(O(N^2), O(2^M))$ since we either store the $\frac{N(N-1)}{2}$ pairwise comparisons or we only store a fixed number of comparisons for each pattern. For datasets with a large number of features, we can use a hash-table to reduce the required storage of the pattern table. In terms of time, the pairwise comparisons is done for all features and objects and thus the time complexity becomes $O(MN^2)$. For Simple Random Sampling, Gupta et al. [36] defined its time and space complexity to be $O(N)$. We used stratified sampling techniques that use simple random sampling to sample from each individual stratum. The stratification parameters are provided and hence, the time and space complexity is also $O(N)$.

In our work, we used the MITOS 2012 dataset that has been widely used in literature. Most of the work applied on this dataset focus on enhancing the accuracy of the classifiers by improving the input features or using advanced machine learning algorithms. In our framework, the main focus is enhancing the quality of the training data. This is achieved by applying the PPS sampler that considers data distribution among the patterns, therefore it can handle data skewness. The samples used in the learning process results in an average F1 measure of 0.84 for both data split and cross validation experiments.

In comparison Noorul et al. [26] proposed a two-phase model that handles class biasness using a balanced convolutional neural network. It is applied on the MITOS 2012 dataset and achieved an average F1 measure of 0.72. Irshad et al. [37] achieved F1 measure of 0.72 while detecting mitosis in breast cancer images. They focused on enhancing data features using selective color channels and employed SVM and decision tree algorithms for the learning. Ciresan et al. [38] achieved F1 measure of 0.66 using the same dataset while applying random undersampling technique with a deep neural network algorithm. Wang et al. [39] improved the features by combining handcrafted and convolutional neural network features. The F1 measure achieved is 0.73. Malon et al. [40] achieved F1 measure of 0.53 while integrating color, texture, and shape features with convolutional neural network extracted features.

5 Conclusion

The proposed sampling method (PPS) is rooted in formal concept analysis. It generates samples using the proportions of data across different binary patterns. The method was evaluated against two well-known sampling methods. The evaluation was performed using a machine-learning case study of breast cancer images. Our method proved to be competitive with the other methods using different learning configurations. Moreover, it perfectly fits the unbalanced data used for classification because it generated a well-balanced sample of these data using the binary distribution. Additionally, it doesn't require any prior knowledge about data or class distribution and it generates the patterns based on all attributes. Furthermore, PPS can be easily improved by employing randomization while selecting the objects from the patterns. This will allow our technique to fit more with machine learning algorithms that suffer from poor generalization such as neural networks. Feature selection algorithms can also be used to reduce the number of features incorporated in the pattern table to reduce the space complexity.

Acknowledgement

This contribution was made possible by NPRP grant #07- 794-1-145 from the Qatar National Research Fund (a member of Qatar Foundation). The statements made herein are solely the responsibility of the authors.

References

[1] Susan G. Komen, Breast Cancer Global Statistics | Susan G. Komen®, (n.d.). http://ww5.komen.org/BreastCancer/Statistics.html (accessed February 8, 2017).

[2] Y. Su, G. Agrawal, J. Woodring, K. Myers, J. Wendelberger, J. Ahrens, Effective and efficient data sampling using bitmap indices, Cluster Comput. 17 (2014) 1081–1100. doi:10.1007/s10586-014-0360-5.

[3] R.W. Bernhard Ganter, Formal Concept Analysis, Mathematical Foundations, Springer, Berlin, 2012. doi:10.1073/pnas.0703993104.

[4] J. Baixeries, M. Kaytoue, A. Napoli, Characterizing functional dependencies in formal concept analysis with pattern structures, Ann. Math. Artif. Intell. (2014) 1–21. doi:10.1007/s10472-014-9400-3.

[5] W. Li, L. Wei, Data Dimension Reduction Based on Concept Lattices in Image Mining, 2009 Sixth Int. Conf. Fuzzy Syst. Knowl. Discov. (2009) 369–373. doi:10.1109/FSKD.2009.685.

[6] Q.X.Q. Xiao, K.Q.K. Qin, Z.G.Z. Guan, T.W.T. Wu, Image mining for robot vision based on concept analysis, 2007 IEEE Int. Conf. Robot. Biomimetics. (2007) 207–212. doi:10.1109/ROBIO.2007.4522161.

[7] L. Yang, Y. Xu, Decision Making with Uncertainty Information Based on Lattice-Valued Fuzzy Concept Lattice, J. Univers. Comput. Sci. 16 (2010) 159–177.

[8] Q. Wan, L. Wei, Approximate concepts acquisition based on formal contexts, Knowledge-Based Syst. 75 (2015) 78–86. doi:10.1016/j.knosys.2014.11.020.

[9] I. Nafkha, A. Jaoua, Using Formal Concept Analysis for Heterogeneous Information Retrieval, Cla 2005. (2005) 107–122. http://ceur-ws.org/Vol-162/paper10.pdf.

[10] S.O. Kuznetsov, Learning of Simple Conceptual Graphs from Positive and Negative Examples, Princ. Data Min. Knowl. Discov. SE - 47. 1704 (1999) 384–391. doi:10.1007/978-3-540-48247-5_47.

[11] B.M. Steele, Sampling Design and Statistical Inference for Ecological Assessment, A Guideb. Integr. Ecol. Assessments. (2001) 79–91.

[12] Y. Tille, Sampling Algorithms, Springer, New York, 2006. doi:10.1007/978-0-387-98135-2.

[13] D.J. Bruse, Statistical Sampling Strategies for Survey of Soil Contamination, Springer

Netherlands, 2011. doi:10.1007/978-90-481-9757-6.

[14] R. Benedetti, F. Piersimoni, P. Postiglione, Sampling Spatial Units for Agricultural Surveys, Springer, Berlin, 2015. doi:10.1007/978-3-662-46008-5.

[15] A.C. Kulshreshtha, Basic Concepts of Sampling- Brief Review : Sampling Designs Survey Design – Issues involved, Second RAP Reg. Work. Build. Train. Resour. Improv. Agric. Rural Stat. Sampl. Methods Agric. Stat. Curr. Pract. SCI, Tehran, Islam. Repub. Iran 10-17 Sept. 2013. (2013).

[16] D. Abid, Segmentation of tumor regions in microscopic images of breast cancer tissue, ProQuest Diss. Theses. (2016) 63.

[17] H. Irshad, A. Veillard, L. Roux, D. Racoceanu, Methods for Nuclei Detection, Segmentation and Classification in Digital Histopathology: A Review. Current Status and Future Potential, IEEE Rev. Biomed. Eng. PP (2013) 1–1. doi:10.1109/RBME.2013.2295804.

[18] M.N. Gurcan, T. Pan, H. Shimada, J. Saltz, Image analysis for neuroblastoma classification: Segmentation of cell nuclei, Annu. Int. Conf. IEEE Eng. Med. Biol. - Proc. (2006) 4844–4847. doi:10.1109/IEMBS.2006.260837.

[19] E. Cosatto, M. Miller, H.P. Graf, J.S. Meyer, Grading nuclear pleomorphism on histological micrographs, Pattern Recognition, 2008. ICPR 2008. 19th Int. Conf. (2008) 1–4. doi:10.1109/ICPR.2008.4761112.

[20] L. Yang, O. Tuzel, P. Meer, D.J. Foran, Automatic image analysis of histopathology specimens using concave vertex graph, Lect. Notes Comput. Sci. (Including Subser. Lect. Notes Artif. Intell. Lect. Notes Bioinformatics). 5241 LNCS (2008) 833–841. doi:10.1007/978-3-540-85988-8_99.

[21] X. Qi, F. Xing, D.J. Foran, L. Yang, Robust segmentation of overlapping cells in histopathology specimens using parallel seed detection and repulsive level set, IEEE Trans. Biomed. Eng. 59 (2012) 754–765. doi:10.1109/TBME.2011.2179298.

[22] J. Chanho, K. Changick, Segmenting Clustered Nuclei Using H-minima Transform-BasedMarker Extraction and\nContour Parameterization, Ieee Trans. Biomed. Eng. 57 (2010) 2600–2604.

[23] S. Ali, A. Madabhushi, An Integrated Region-, Boundary-, Shape-Based Active Contour for Multiple Object Overlap Resolution in Histological Imagery, Eee Trans. Med. Imaging. 31 (2012) 1448–1460.

[24] A.M. Khan, H. El-Daly, E. Simmons, N.M. Rajpoot, HyMaP: A hybrid magnitude-phase approach to unsupervised segmentation of tumor areas in breast cancer histology images., J. Pathol. Inform. 4 (2013) S1. doi:10.4103/2153-3539.109802.

[25] K. Sirinukunwattana, S.E.A. Raza, Y.W. Tsang, D.R.J. Snead, I.A. Cree, N.M. Rajpoot, Locality Sensitive Deep Learning for Detection and Classification of Nuclei in Routine Colon Cancer Histology Images, IEEE Trans. Med. Imaging. 35 (2016) 1196–1206. doi:10.1109/TMI.2016.2525803.

[26] N. Wahab, A. Khan, Y.S. Lee, Two-phase deep convolutional neural network for reducing class skewness in histopathological images based breast cancer detection, Comput. Biol. Med. (2017). doi:10.1016/j.compbiomed.2017.04.012.

[27] E. Reinhard, M. Ashikhmin, B. Gooch, P. Shirley, Color transfer between images, IEEE Comput. Graph. Appl. 21 (2001) 34–41. doi:10.1109/38.946629.

[28] M. Macenko, M. Niethammer, J.S. Marron, D. Borland, J.T. Woosley, X. Guan, C. Schmitt,

N.E. Thomas, A method for normalizing histology slides for quantitative analysis, Proc. - 2009 IEEE Int. Symp. Biomed. Imaging From Nano to Macro, ISBI 2009. (2009) 1107–1110. doi:10.1109/ISBI.2009.5193250.

[29] A. Khan, N. Rajpoot, D. Treanor, D. Magee, A Non-Linear Mapping Approach to Stain Normalisation in Digital Histopathology Images using Image-Specific Colour Deconvolution, IEEE Trans. Biomed. Eng. XX (2014) 1–1. doi:10.1109/TBME.2014.2303294.

[30] A. Graham, A. Kamen, L. Grady, P. Khurd, N. Navab, J. Ni, C. Bahlmann, E. Krupinski, A. Chekkoury, J. Johnson, A. Patel, R. Weinstein, M. Singh, M. Groher, Automated malignancy detection in breast histopathological images, SPIE Med. Imaging. 8315 (2012) 831515. doi:10.1117/12.911643.

[31] M. Peikari, M.J. Gangeh, J. Zubovits, G. Clarke, A.L. Martel, Triaging diagnostically relevant regions from pathology whole slides of breast cancer: A texture based approach, IEEE Trans. Med. Imaging. 35 (2016) 307–315. doi:10.1109/TMI.2015.2470529.

[32] A. Qu, J. Chen, L. Wang, J. Yuan, F. Yang, Q. Xiang, N. Maskey, G. Yang, J. Liu, Y. Li, Segmentation of Hematoxylin-Eosin stained breast cancer histopathological images based on pixel-wise SVM classifier, Sci. China Inf. Sci. 58 (2015) 1–13. doi:10.1007/s11432-014-5277-3.

[33] E. Rezk, S. Babi, F. Islam, A. Jaoua, Uncertain Training Data Set Conceptual Reduction : A Machine Learning Perspective, in: FUZZ-IEEE, “in press,” Vancouver, 2016.

[34] C. Goutte, E. Gaussier, A Probabilistic Interpretation of Precision, Recall and F -Score, with Implication for Evaluation, 27th Eur. Conf. IR Res. ECIR 2005, Santiago Compost. 3408 (2005) 345–359. doi:10.1007/b107096.

[35] L. Zhang, P.N. Suganthan, A survey of randomized algorithms for training neural networks, Inf. Sci. (Ny). 364–365 (2016) 146–155. doi:10.1016/j.ins.2016.01.039.

[36] P. Gupta, G.P. Bhattacharjee, An Efficient Algorithm For Random Sampling Without Replacement, in: Found. Softw. Technol. Theor. Comput. Sci., Bangalore, India, 1984. doi:10.1007/3-540-13883-8.

[37] H. Irshad, Automated mitosis detection in histopathology using morphological and multi-channel statistics features, J. Pathol. Inform. 4 (2013) 10. doi:10.4103/2153-3539.112695.

[38] D.C. Ciresan, A. Giusti, L.M. Gambardella, J. Schmidhuber, Mitosis Detection in Breast Cancer Histology Images using Deep Neural Networks, Med. Image Comput. Comput. Interv. (MICCAI 2013). (2013) 411–418.

[39] H. Wang, A. Cruz-Roa, A. Basavanhally, H. Gilmore, N. Shih, M. Feldman, J. Tomaszewski, F. Gonzalez, A. Madabhushi, Mitosis detection in breast cancer pathology images by combining handcrafted and convolutional neural network features, J. Med. Imaging. 1 (2014) 34003. doi:10.1117/1.JMI.1.3.034003.

[40] C. Malon, E. Cosatto, Classification of mitotic figures with convolutional neural networks and seeded blob features, J. Pathol. Inform. 4 (2013) 9. doi:10.4103/2153-3539.112694.